PNAS
www.pnas.org

Supplementary Information for:

Epigenetic state determines inflammatory sensing in neuroblastoma

Adam J. Wolpaw, Liron D. Grossmann, Jessica L. Dessau, May M. Dong, Bailey J. Aaron, Patricia A. Brafford, Darya Volgina, Guillem Pascual-Pasto, Alba Rodriguez-Garcia, Yasin Uzun, Marie Arsenian-Henriksson, Daniel J. Powell Jr, Kristopher R. Bosse, Andrew Kossenkov, Kai Tan, Michael D. Hogarty, John M. Maris, Chi V. Dang

Correspondence to:
Chi V. Dang
cdang@lcr.org
Adam J. Wolpaw
Wolpawa@chop.edu

This PDF file includes:

Supplementary Materials and Methods

Reagents

Sources and concentrations of reagents not specified in the method section are listed in Table S3. Calf thymus DNA was transfected with jetPRIME transfection reagent (VWR 89129-920). Qiagen FlexiTube siRNAs were transfected using Lipofectamine™ RNAiMax Transfection reagent (13778150) according to the manufacturer's protocol. The Luciferase Assay System (E1501) was purchased from Promega and used according to the manufacturer's instructions.

Plasmids

NF-κB pNifty2-Luc (Invivogen) was transfected into cell lines using Lipofectamine™ 3000 transfection reagent (L3000008) followed by zeocin selection. Myc-DDK-PRRX1a and Myc-DDK-TLR3 were purchased from Origene (RC213276, RC210497). TLR3 was transfected using Lipofectamine™ 3000 and selected with G418. PRRX1a was cloned into the pLVX-TetOne (Takara 631847). Final plasmid identity was validated by sequencing. Lentivirus was produced from the PRRX1a plasmid and the analogous luciferase control and cells were infected as previously described (1). Infected cells were selected with puromycin. Lentiviral particles for MART-1 expressed from an EF1a promoter with an IRES-eGFP were purchased from Genecopoeia (G0616-Lv225). GFP control was expressed using a lentiviral vector with an EF1a promoter and IRES-eGFP.

Western blots

Cells were lysed on ice using M-PER (Thermo Scientific 78501) with phosphatase inhibitor cocktails 2 and 3 (Sigma Aldrich P5726, P0044) and a protease inhibitor cocktail from Promega (G6521) then scraped and cleared by centrifugation at 4°C. Tumors were minced with a single edge blade and suspended in RIPA buffer (Prometheus, 18-415) with the same protease and phosphatase inhibitors as was used for cell lines. Samples were then homogenized using a gentleMACS Octo Dissociator and M Tubes according to the manufacturer's recommendations. Protein was quantified using the DC Protein Assay (Bio-Rad) then electrophoresed using Criterion TGX gels (Bio-Rad) and transferred to nitrocellulose membranes via iBlot2. Membranes were blocked in Odyssey blocking buffer. Primary antibodies used for immunoblotting are listed in Table S3. They were diluted in TBS-T with 5% bovine serum albumin. Immunoblots were visualized by an Odyssey CLx (LI-COR).

Flow cytometry

For cell line analysis, cells were trypsinized and resuspended in PBS with 2% FBS at 1x10^6 cells/mL, then incubated with antibodies (1:100, see Table S3) at 37*C for 30 minutes. Cells were washed twice with 2% FBS in PBS, then resuspended in 50% accutase (Sigma A6964) and 50% PBS with 2% FBS. Flow cytometry was executed using a Guava EasyCyte flow cytometer (Luminex). Tumors were minced with a single edge blade, incubated in RPMI with 55U/mL of collagenase (Fisher, 17104019), 0.8U/mL of dispase (Sigma D4693), and 1000U/mL of DNAse (Sigma 10104159001), and homogenized with a gentleMACS Octo Dissociator with a C Tube. Cells were strained to ensure a single cell suspension and red cells lysed (Invitrogen 00-4300-54). Cells were counted and 4 million cells stained in 100uL using antibodies listed in Table S3. Flow cytometry was executed using a FACSymphony flow cytometer. Data were analyzed in FlowJo. Live cells were identified using LIVE/DEAD™ Fixable Aqua Dead Cell Stain Kit (Thermofisher L34965). Total CD45+ cells were defined as CD45+/CD147-. NK cells were defined as CD45+/CD49b+/NKp46+, dendritic cells as CD45+/CD19-/TCRβ-/MHC2+/CD11c+/CD11b+, macrophages as CD45+/CD19-/TCRβ-/F480+/CD11c-/MHC2+, monocytic myeloid-derived suppressor cells (M-MDSCs) as CD45+/CD19-/TCRβ-/CD11b+/Ly6c+, and polymorphonuclear myeloid-derived suppressor cells (PMN-MDSCs) as CD45+/CD19-/TCRβ-/CD11b+/Ly6g+.

Quantitative PCR

RNA was extracted using the Qiagen RNeasy Plus mini kit (74134) after homogenization by centrifugation in QIAShredder (79656) microcentrifuge tubes. For qPCR, RNA was reverse transcribed with a TaqMan Reverse Transcription Reagent Kit (Applied Biosystems N8080234,

using oligo(dT)). Relative transcript abundance was obtained using Power SYBR Green Master Mix (ThermoFisher) using the QuantStudio 6 Flex Real-Time PCR System using the primers listed in Table S3, RPLP0 was used as a normalization control.

Cell migration assays
Conditioned media was prepared by transferring cells to serum-free media with or without 30μg/mL of poly (I:C) for 24 hours, then collecting and centrifuging at 500g for 5 minutes before transferring 100 μL to the lower chamber of a Corning Transwell® plate (3388) with 5μm pore size filters. THP-1 cells (2x10^5) were seeded in the upper chamber and allowed to migrate for 2 hours. Migrated cells were quantified by counting with a ViCell BLU Cell Viability Analyzer (Beckman Coulter).

Immunohistochemistry
Tissue staining was performed by the Wistar Histotechnology Facility. Tumor were dissected, fixed in formalin, paraffin embedded, and sectioned. Slides were deparaffinized and antigen retrieval was performed with DAKO Target Retrieval Solution (#S2367) followed by immersion in 3% hydrogen peroxide, permeabilization with TX-100, and blocking with 2.5% horse serum. Slides were stained with pSTAT1 antibody (Cell Signaling 9167) at 1:100 overnight at 4°C and developed with horse anti-rabbit IgG secondary (Vector Laboratories MP-7401) and DAB. Slides were counterstained with hematoxylin. Images were captured using a Nikon 80i Upright microscope using the 10x lens. Entire sections were examined and representatively staining sections chosen for image capture.

ATAC-seq
CHP-212, GI-ME-N, IMR-5, and SK-N-DZ cells were enzymatically dissociated and counted, then 100,000 cells were pelleted and resuspended in 50% FBS, 40% growth media, and 10% DMSO. Cells were cooled slowly to minimize cell lysis with freezing and then shipped on dry ice to Active Motif (Carlsbad, CA). The cells were then thawed in a 37°C water bath, pelleted, washed with cold PBS, and tagmented as previously described (2), with some modifications based on (3). Briefly, cell pellets were resuspended in lysis buffer, pelleted, and tagmented using the enzyme and buffer provided in the Nextera Library Prep Kit (Illumina). Tagmented DNA was then purified using the MinElute PCR purification kit (Qiagen), amplified with 10 cycles of PCR, and purified using Agencourt AMPure SPRI beads (Beckman Coulter). Resulting material was quantified using the KAPA Library Quantification Kit for Illumina platforms (KAPA Biosystems), and sequenced with PE42 sequencing on the NextSeq 500 sequencer (Illumina). Data for Kelly and SK-N-AS cells were downloaded from GSE138315 (4) for statistical analysis of differential accessibility at genes in the TLR3 pathway and the Antigen Presentation and Processing pathway. ATAC-seq data for all 6 cell lines were then aligned using bowtie (5) against hg19 version of the human genome and HOMER (6) was used to generate bigwig files and call significant peaks using "-style dnase" option. Differential signal analysis was performed on raw ATAC-seq signals for 500bp around genes' TSS derived using HOMER over Ensemble transcriptome. Significance of pair-wise differences between cell line groups was estimated using DESeq2 (7) and results with nominal p-value <0.05 were considered significant. Tracks were visualized using R2: Genomics Analysis and Visualization Platform (http://r2.amc.nl). For visualization of tracks, data for Kelly and SK-N-AS was obtained from within R2. For the newly generated data, reads were aligned using the BWA algorithm (mem mode; default settings). Duplicate reads were removed, only reads mapping as matched pairs and only uniquely mapped reads (mapping quality >= 1) were used for further analysis. Alignments were extended in silico at their 3'-ends to a length of 200 bp and assigned to 32-nt bins along the genome. The resulting histograms (genomic "signal maps") were stored in bigwig files and uploaded to R2 for visualization.

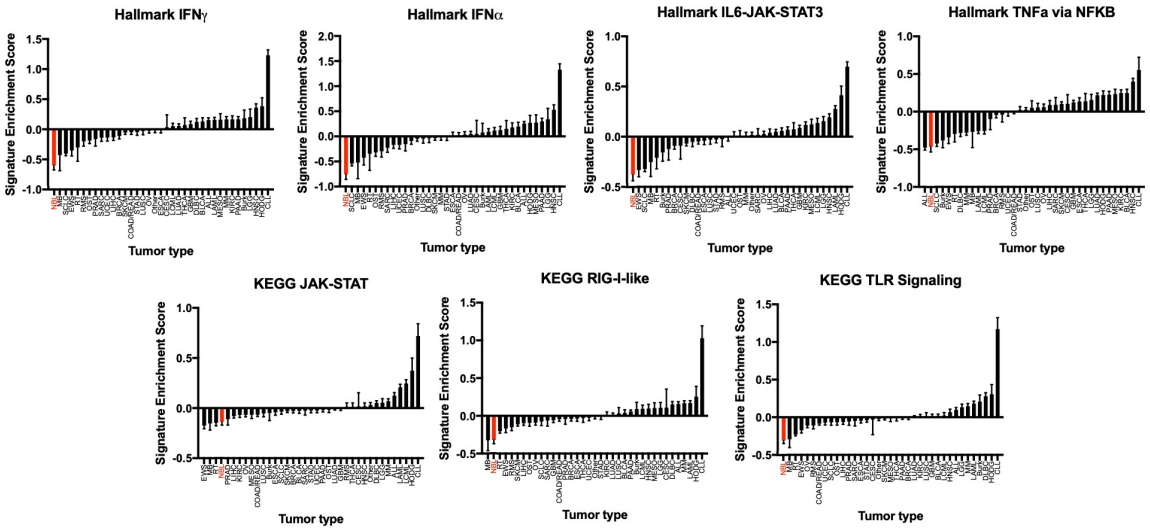

Fig. S1. Enrichment scores of inflammatory signatures in the CCLE
Enrichment scores across 7 different inflammatory signatures for cell lines in the CCLE, with neuroblastoma highlighted in red. Data downloaded from the Broad CCLE portal (https://sites.broadinstitute.org/ccle). Abbreviations: ALL = acute lymphoblastic leukemia, BRCA = breast invasive carcinoma, Burk = Burkitt lymphoma, CESC = cervical squamous cell carcinoma and endocervical adenocarcinoma, CLL = chronic lymphocytic leukemia, COAD/READ = colon adenocarcinoma/rectum adenocarcinoma, DLBCL = lymphoid neoplasm diffuse large B-cell lymphoma, ESCA = esophageal carcinoma, EWS = Ewing sarcoma, GBM = glioblastoma multiforme, HODG = Hodgkin's lymphoma, HNSC = head and neck squamous cell carcinoma, KIRC = kidney renal clear cell carcinoma, LAML = acute myeloid leukemia, LCML = chronic myelogenous leukemia, LGG = brain lower grade glioma, LIHC = liver hepatocellular carcinoma, LUAD = lung adenocarcinoma, LUSC = lung squamous cell carcinoma, MB = medulloblastoma, MESO = mesothelioma, MM = multiple myeloma, NBL = neuroblastoma, OST = osteosarcoma, OV = ovarian serous cystadenocarcinoma, PAAD = pancreatic adenocarcinoma, PRAD = prostate adenocarcinoma, RMS = rhabdomyosarcoma, RT = rhabdoid tumor, SARC = sarcoma, SCLC = small cell lung carcinoma, SKCM = skin cutaneous melanoma, STAD = stomach adenocarcinoma, THCA = thyroid carcinoma, UCEC = uterine corpus endometrial carcinoma. Error bars represent SEM among cell lines from the same tumor type.

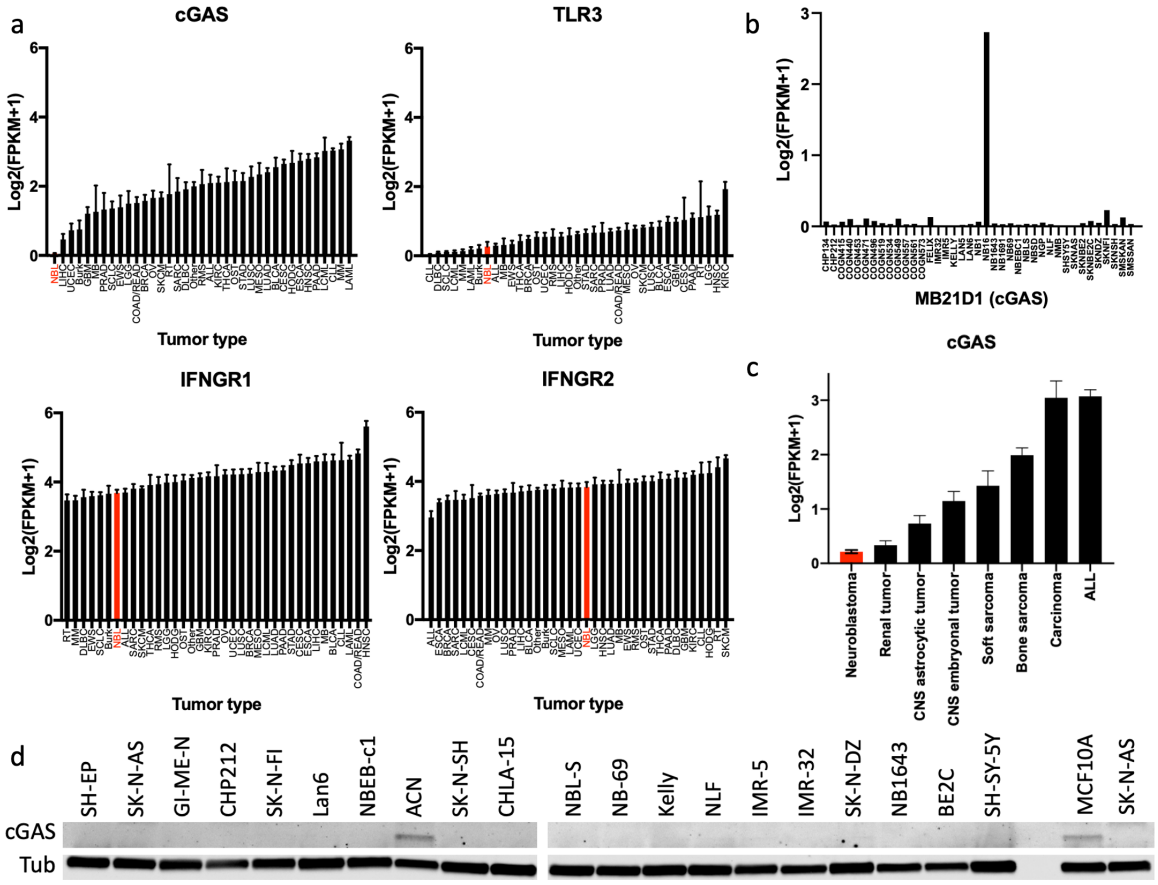

Fig. S2. Expression of inflammatory sensors in the CCLE and in neuroblastoma cell lines
a) Expression of the indicated genes across tumor types in the CCLE. Data downloaded from the Broad CCLE portal (https://sites.broadinstitute.org/ccle). See Figure S1 for abbreviations. b) Expression of *cGAS* in a neuroblastoma cell line RNA-seq dataset (GSE89413 (8)). c) Expression of *cGAS* in a pediatric tumor xenograft dataset, separated by tumor type as indicated. Data from (9), downloaded from PedcBioPortal (https://pedcbioportal.kidsfirstdrc.org). d) Western blot demonstrating expression of cGAS in the 20 neuroblastoma cell lines used in the current study. MCF10A cells are shown as a positive control for cGAS. Error bars represent SEM among cell lines or tumors from the same tumor type.

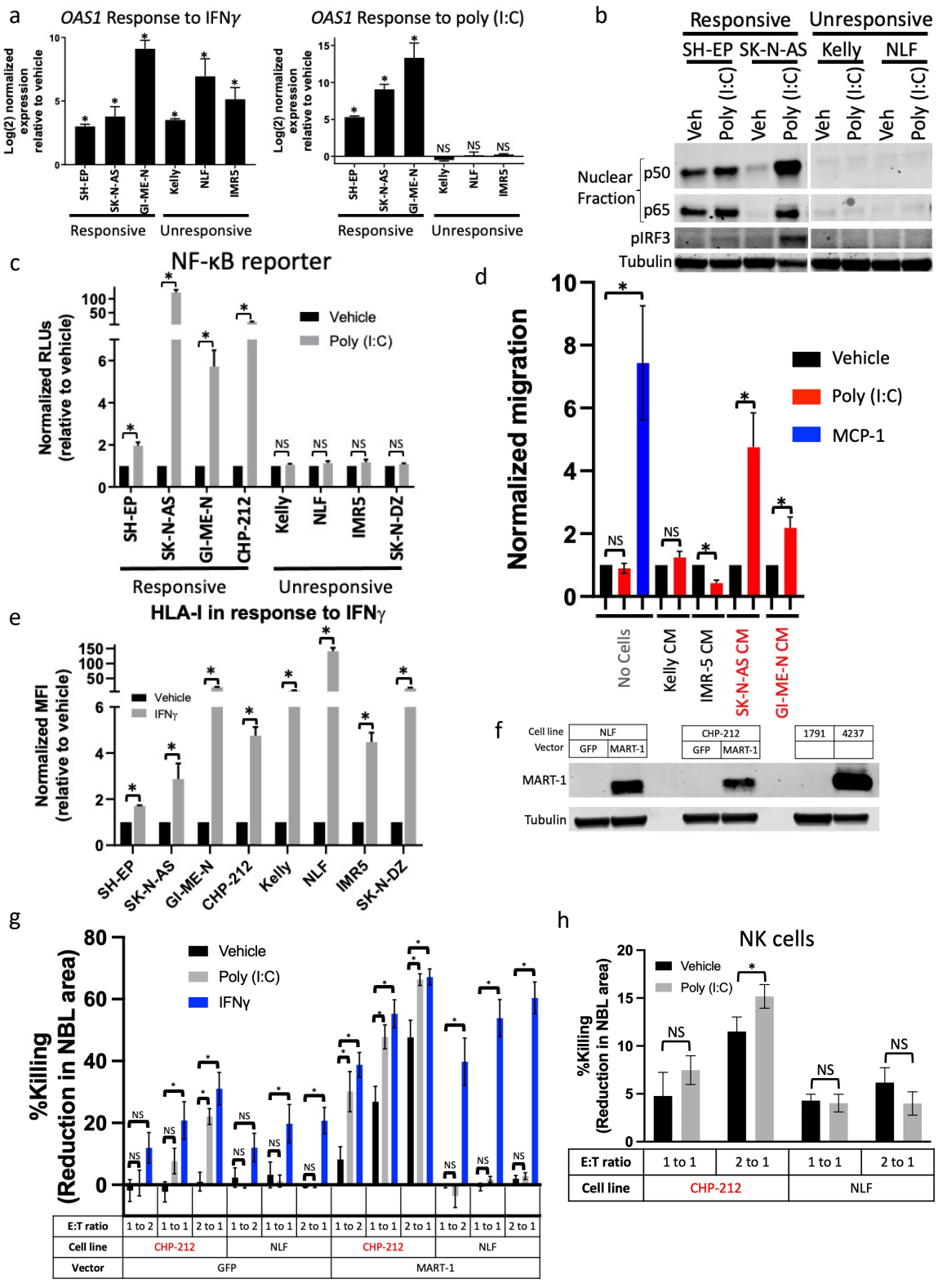

Fig. S3. Additional metrics of differential response to dsRNA in neuroblastoma cell lines
a) Change in expression of *OAS1* as measured by qPCR in the indicated neuroblastoma cell lines after treatment with 20ng/mL IFNγ for 24 hours (left) or 30μg/mL of poly (I:C) (right) compared to vehicle control. b) Change in the phosphorylation of IRF3 and the nuclear

localization of NF-κB subunits p50 and p65 after treatment of the indicated cell lines with vehicle control or poly (I:C) for 24 hours. c) Luminescence normalized to vehicle only control in the indicated cell lines transfected with an NF-κB reporter after treatment with vehicle control or poly (I:C) for 24 hours. d) Change in migration of THP-1 cells from the upper chamber across a filter with 5μm pore diameter with conditioned media (CM) from the indicated treatments and cell lines in the lower chamber. MCP-1 was used at 50nM. e) Surface expression of HLA-I, measured by flow cytometry, in the indicated neuroblastoma cell lines after treatment with vehicle control or IFNγ for 24 hours. f) Western blot showing expression of MART-1 in NLF and CHP-212 cells after expression of GFP control or MART-1. MART-1 negative (1791) and MART-1 positive (4237) melanoma cells are shown as controls. g) Change in killing of neuroblastoma cells exogenously expressing either GFP control or MART-1 after culture with MART-1 transgenic tTCR-transfected T cells. Neuroblastoma cells were treated with the indicated agonists for 24 hours then washed and cultured with the T cells. E:T ratio is the effector (T cell) to target (neuroblastoma) ratio. Killing was calculated by microscopy-based detection of change in cell area. h) Change in killing of neuroblastoma cells exogenously expressing GFP after culture with NK cells. Neuroblastoma cells were treated with the indicated agonists for 24 hours then washed and cultured with the NK cells. E:T ratio is the effector (NK cell) to target (neuroblastoma) ratio. Killing was calculated by microscopy-based detection of change in cell area. Two-tailed paired T-test between biological replicates except in (g) where an ANOVA was used, *$p<0.05$. Error bars represent SEM between biological replicates. Western blots are representative of results from at least three separate experiments.

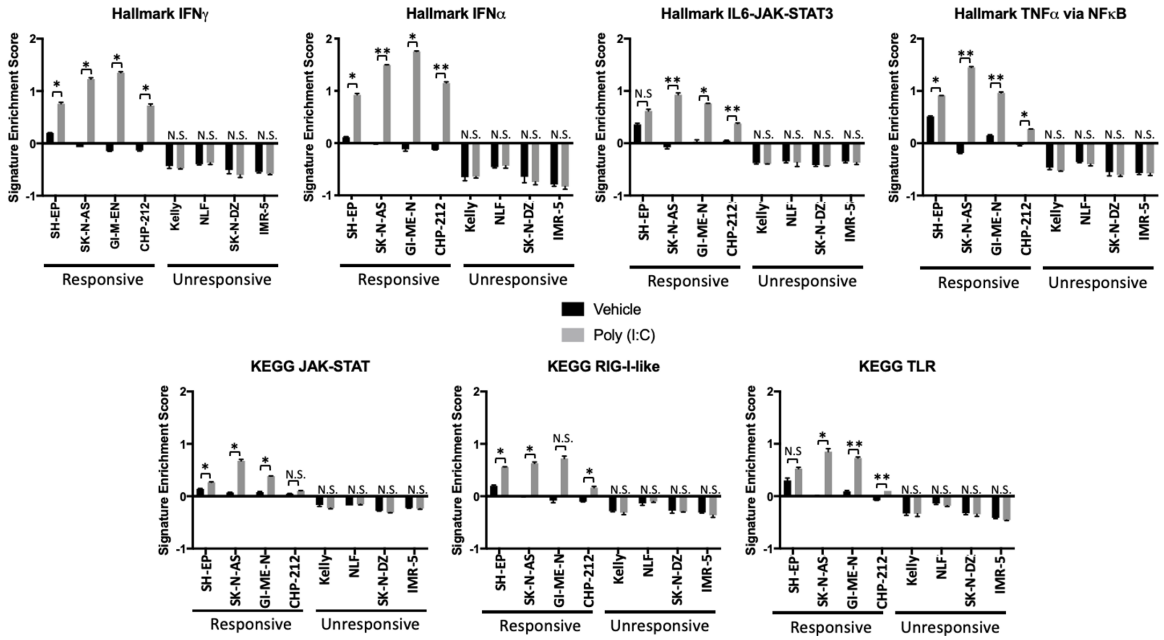

Fig. S4. Changes in gene expression signatures in neuroblastoma cell lines after treatment with poly (I:C)

Relative enrichment of 7 different inflammatory signaling signatures in the indicated cell lines treated with vehicle or 30μg/mL of poly (I:C) for 24 hours as measured by Quantseq. Two-tailed paired T-test between biological replicates showing an increase in the signature upon treatment, *p<0.05, **p<0.01. Error bars represent SEM between biological replicates.

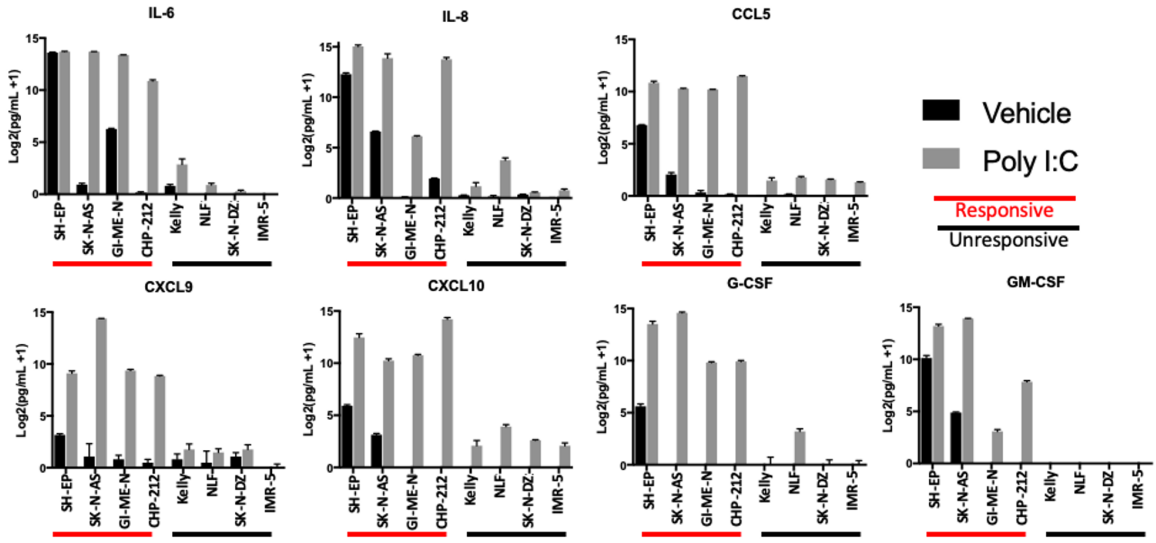

Fig. S5. Changes in cytokine secretion upon treatment with poly (I:C)
Change in cytokines in supernatant of the indicated cell lines after treatment with vehicle or 30μg/mL of poly (I:C) for 24 hours. Comparison between the level of each responsive cell line after treatment is significantly different than that of each unresponsive line ($p<0.05$) for all cytokines shown based on an ANOVA. Error bars represent SEM between biological replicates.

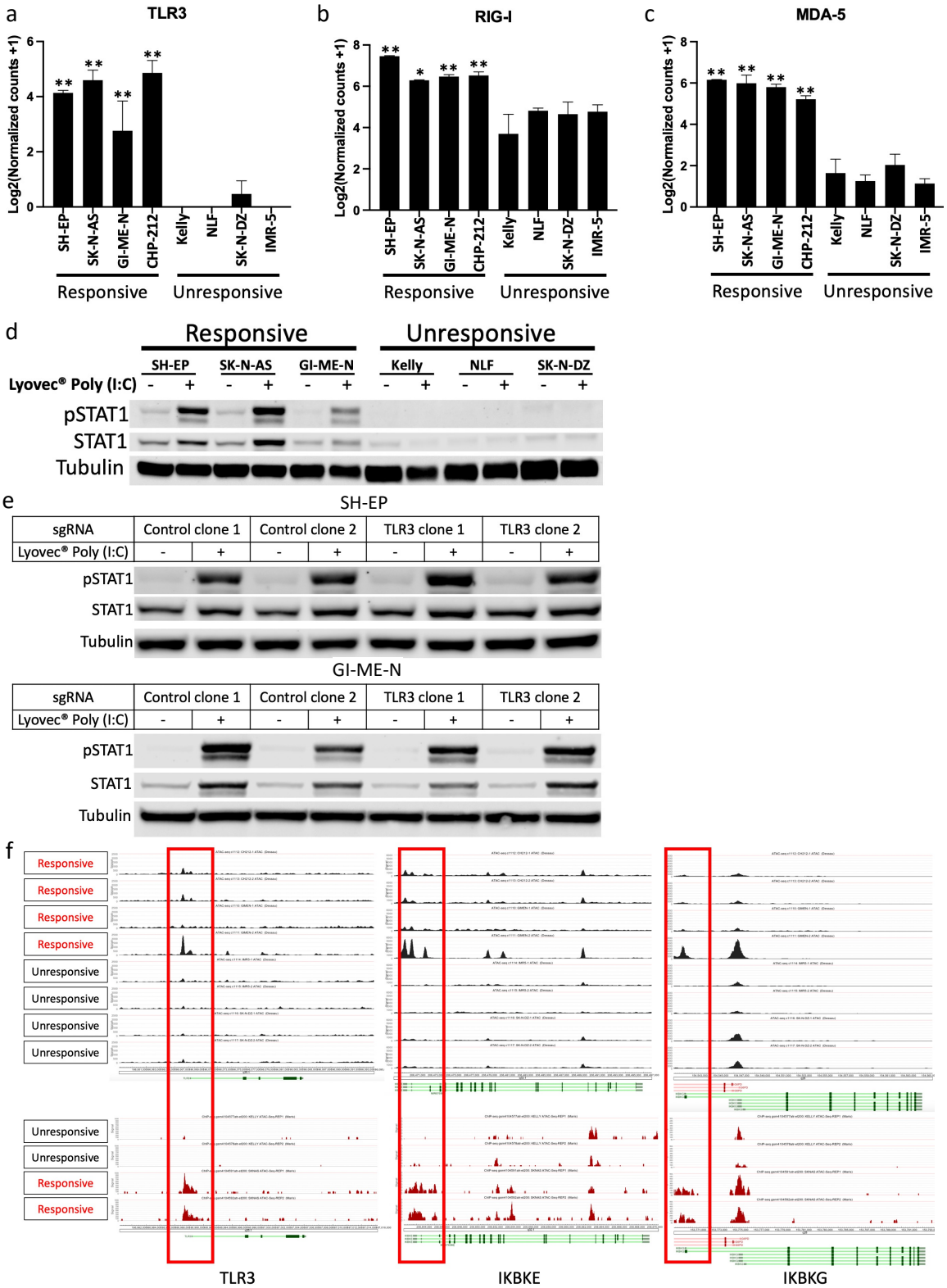

Fig. S6. Intracellular and extracellular dsRNA sensors are expressed and functional only in poly (I:C)-responsive lines

Transcript expression as measured by Quantseq of *TLR3* (a), *RIG-I* (b), and *MDA-5* (c) in the indicated cell lines. ANOVA comparing responsive lines to the set of unresponsive lines, *p<0.05, **p<0.01. Error bars represent SEM between biological replicates. d) Western blot showing the

change in pSTAT1 after treatment with 5µg/mL of poly (I:C) complexed with Lyovec® transfection reagent for 24 hours to test the response to intracellular dsRNA in three poly (I:C) responsive and three unresponsive cell lines. e) Western blot showing the change in pSTAT1 after treatment with poly (I:C) complexed with Lyovec® transfection reagent for 24 hours in the two indicated poly (I:C) responsive cell lines with or without CRISPR-Cas9-mediated knockout of TLR3. f) ATAC-seq tracks for the three indicated genes that were significantly more accessible in the responsive cell lines. Tracks were visualized with in R2 (http://r2.amc.nl). Red box indicates the promoter region of each gene. Two independent replicates are displayed for each cell line. The samples, in order from the top, are CHP-212_rep1, CHP-212_rep2, GI-ME-N_rep1, GI-ME-N_rep2, IMR-5_rep1, IMR5_rep2, SK-N-DZ_rep1, SK-N-DZ_rep2, Kelly_rep1, Kelly_rep2, SK-N-AS_rep1, SK-N-AS_rep2. Y-axis represents the number of reads per 20 million mapped reads.

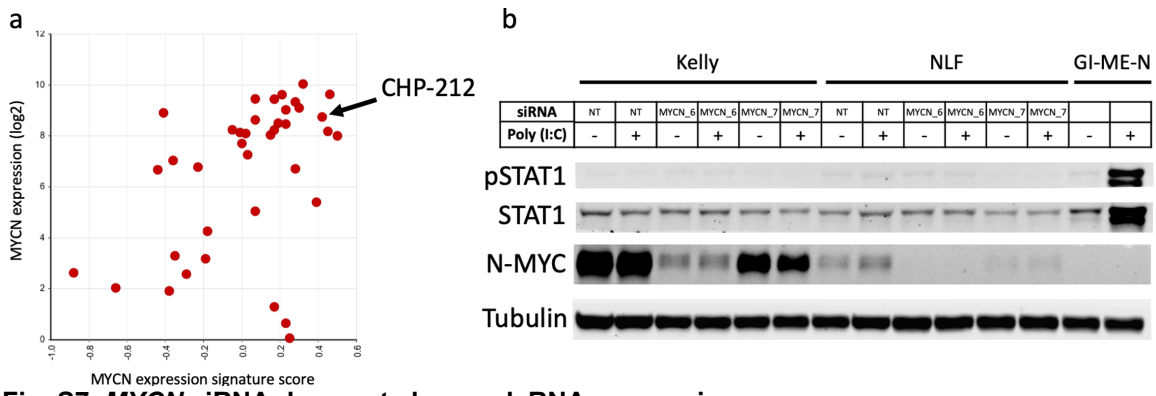

Fig. S7. *MYCN* siRNA does not change dsRNA responsiveness

a) Comparison of *MYCN* expression and relative enrichment score of a functional MYCN signature (10). Data from GSE89413 (8), obtained from and analyzed in R2 (http://r2.amc.nl). b) Western blot showing changes in pSTAT1, STAT1, and MYCN when Kelly or NLF cells were treated with either a control siRNA or one of two different siRNAs targeting *MYCN* for 72 hours, at which point they were then treated with either vehicle or 30μg/mL of poly (I:C) for 24 hours.

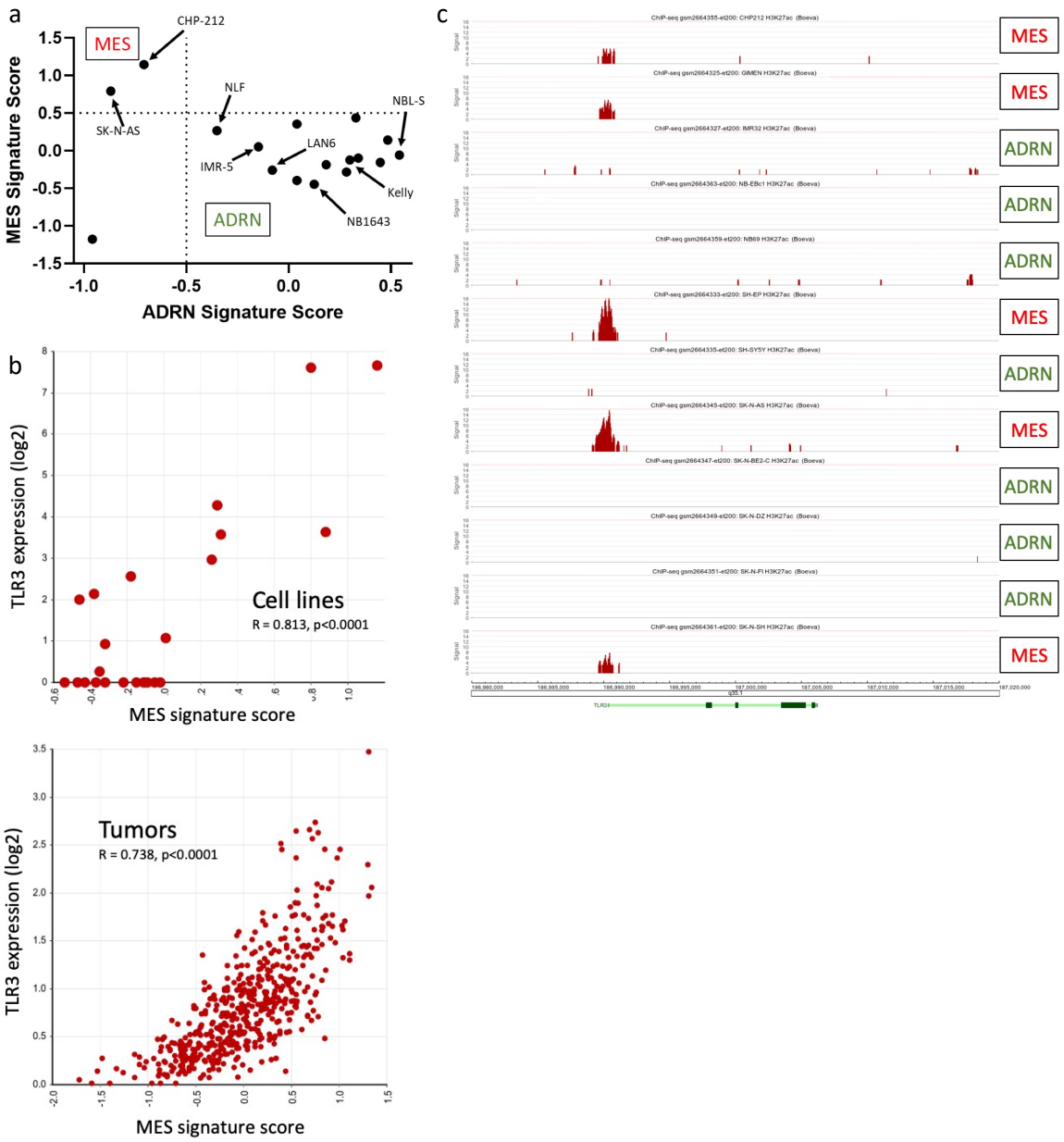

Fig. S8. Classification of neuroblastoma cell lines and relationship between TLR3 and MES expression signature

a) Comparison of MES and ADRN gene expression signature scores for cell lines used in the current study, data from GSE89413 (8), signatures from (11). Dotted lines indicate classification cutoffs used. b) Top - comparison of *TLR3* expression and the relative enrichment score of the MES signature in 23 neuroblastoma cell lines. Data from GSE28019, obtained from and analyzed in R2 (http://r2.amc.nl). Bottom - comparison of *TLR3* expression and the relative enrichment score of the MES signature in 498 neuroblastoma tumors. Data from (12), obtained from and analyzed in R2 (http://r2.amc.nl). c) ChIP-seq for H3K27Ac in the 12 indicated neuroblastoma cell lines surrounding the TLR3 locus. Data from (13), obtained from and analyzed in R2 (http://r2.amc.nl). Y-axis represents the number of reads per 20 million mapped reads.

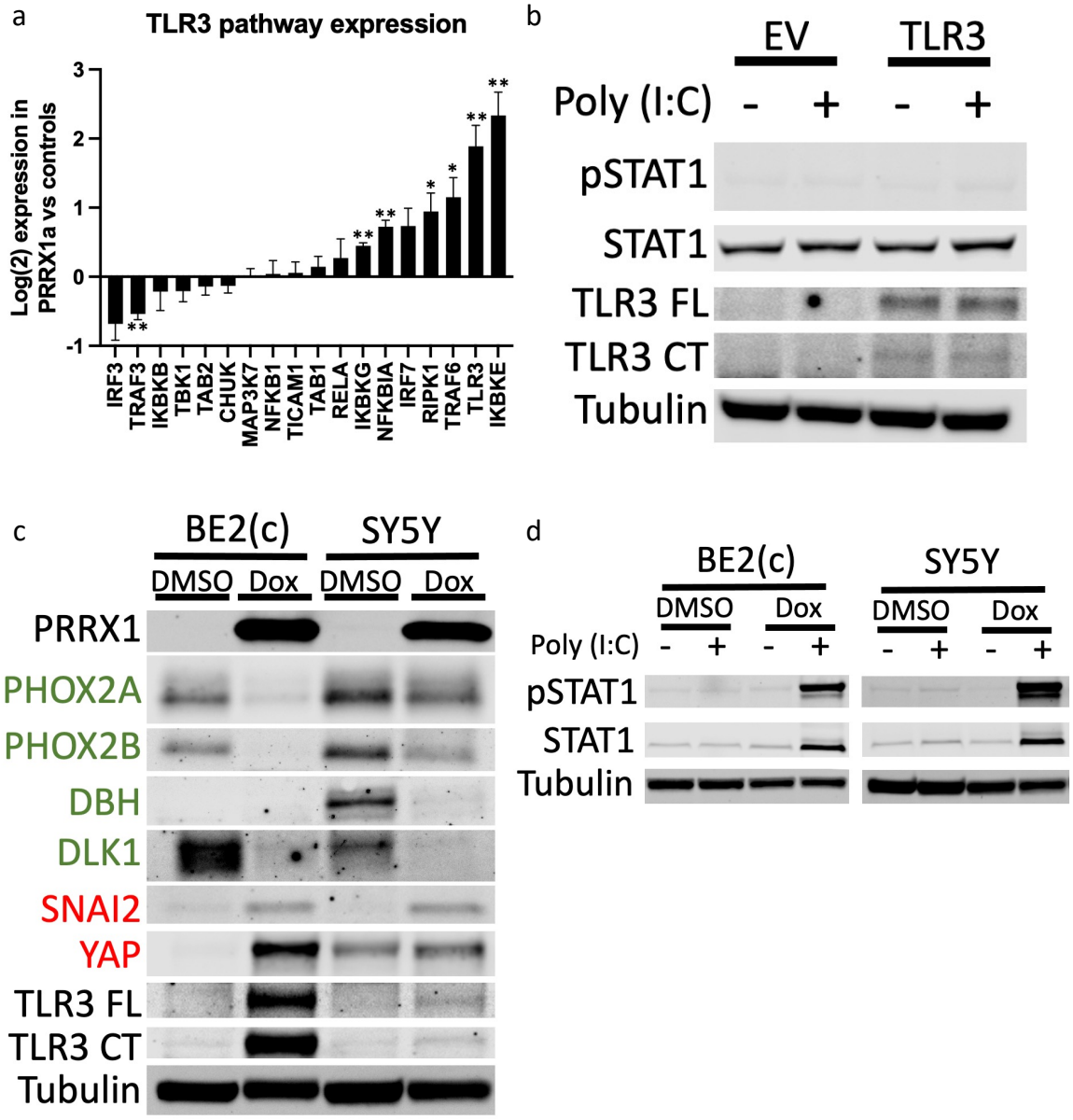

Fig. S9. TLR3 pathway expression and response changes with PRRX1 expression
a) Difference in transcript expression as measured by Quantseq of genes in the TLR3 signaling pathway between BE2(c) cells induced to express PRRX1 and controls either not induced or induced to express luciferase. Cells were treated with vehicle or doxycycline for 14 days. b) Western blot showing change in pSTAT1, total STAT1, and TLR3 after treatment with 30μg/mL of poly (I:C) for 24 hours with or without expression of exogenous TLR3 in BE2(c) cells. Both the full length (FL) and an active C-terminal fragment (CT) of TLR3 are shown. c) Western blot showing changes in the adrenergic markers PHOX2A, PHOX2B, DBH, and DLK1, the mesenchymal markers SNAI2 and YAP1, and TLR3 with or without inducible expression of PRRX1 for 7 days in the indicated cells lines. d) Western blot showing changes in pSTAT1 and total STAT1 in the indicated cells lines after PRRX1 inducible cell lines were treated with vehicle or doxycycline (Dox) for 7 days, then treated with vehicle or poly (I:C) for 24 hours. Western blots are representative of results from at least three separate experiments. Two-tailed paired T-test between responsive and unresponsive, *p<0.05, **p<0.01. Error bars represent SEM between biological replicates.

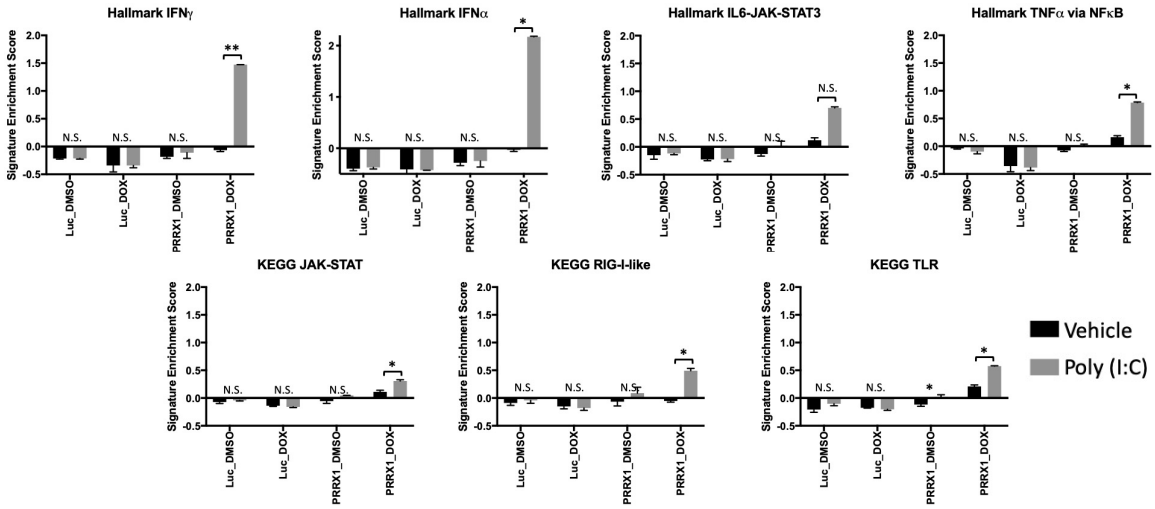

Fig. S10. Effect of PRRX1 expression on the change in gene expression signatures after treatment with poly (I:C)

Relative enrichment of 7 different inflammatory signaling signatures in BE2(c) cells expressing inducible Luciferase control (Luc) or PRRX1 treated with vehicle or doxycycline for 14 days, then treated with vehicle or 30μg/mL of poly (I:C) for 24 hours as measured by Quantseq. Two-tailed paired T-test between biological replicates showing an increase in the signature upon treatment, *p<0.05, **p<0.01. Error bars represent SEM between biological replicates.

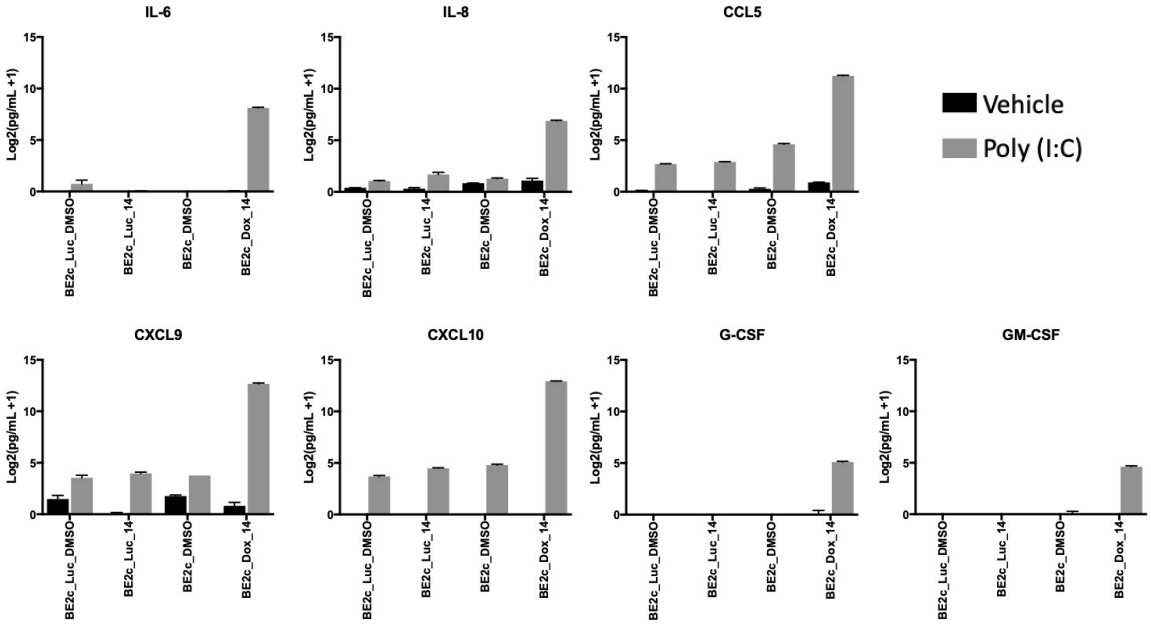

Fig. S11. Changes in cytokine secretion upon treatment with poly (I:C) after PRRX1 expression

Change in cytokines in supernatant of BE2(c) cells expressing inducible Luc or PRRX1 treated with vehicle or dox for 14 days, then treated with vehicle or 30μg/mL of poly (I:C) for 24 hours measured as Log2(pg/mL+1). Comparison between the level of PRRX1 expressing cells treated with dox and poly I:C is significantly different from all other samples ($p<0.01$) for each cytokine shown using an ANOVA. Error bars represent SEM between biological replicates.

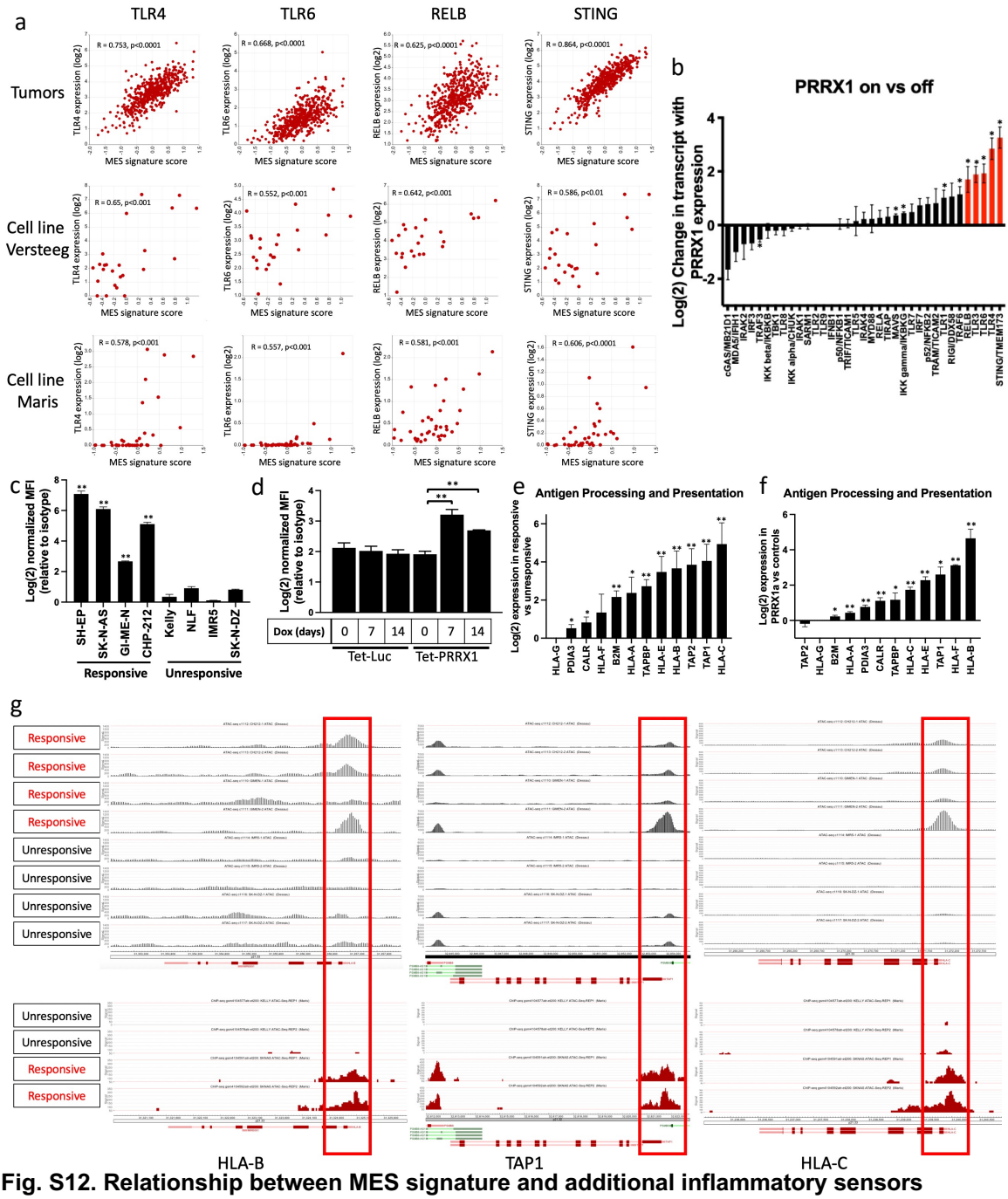

Fig. S12. Relationship between MES signature and additional inflammatory sensors

a) Comparison of *TLR4, TLR6, RELB, and STING* expression and the relative enrichment score of the MES signature (11). Top row shows relationship in 498 neuroblastoma tumors (data from (12)). Middle row shows relationship in 23 neuroblastoma cell lines (data from GSE28019). Bottom row shows relationship in 39 neuroblastoma cell lines (data from (8)). All data obtained from and analyzed in R2 (http://r2.amc.nl). b) Change in expression of receptors, adaptors/signaling proteins, and effector transcription factors involved in TLR and other pattern recognition receptor signaling with PRRX1 expression in BE2(c) cells. Cells induced to express PRRX1 were compared to three pooled control conditions (luciferase control vector on/off, PRRX1 vector off). Data from Quantseq analysis. Transcripts highlighted in red were significantly correlated with the MES signature in tumors and in two cell line datasets (shown in panel (a)). c) Depiction of the basal surface expression of HLA-I as measured by flow cytometry in the

indicated cells lines. Each responsive cell line is significantly different from each unresponsive line ($p<0.01$). d) Depiction of the surface expression of HLA-I as measured by flow cytometry in BE2(c) cells induced to express either PRRX1 or a luciferase (Luc) control. e) Difference in basal expression of genes involved in antigen processing and presentation between responsive and unresponsive cell lines as measured by Quantseq. f) Difference in expression of genes involved in antigen processing and presentation between BE2(c) cells induced to express PRRX1 and controls either not induced or induced to express luciferase as measured by Quantseq. g) ATAC-seq tracks for the three indicated genes that were significantly more accessible in the responsive cell lines. Tracks were visualized with in R2 (http://r2.amc.nl). Red box indicates the promoter region of each gene. Two independent replicates are displayed for each cell line. The samples, in order from the top, are CHP-212_rep1, CHP-212_rep2, GI-ME-N_rep1, GI-ME-N_rep2, IMR-5_rep1, IMR5_rep2, SK-N-DZ_rep1, SK-N-DZ_rep2, Kelly_rep1, Kelly_rep2, SK-N-AS_rep1, SK-N-AS_rep2. Y-axis represents the number of reads per 20 million mapped reads. For (b), (e), (f), two-tailed T-test, for (c) and (d) ANOVA, *$p<0.05$, **<0.01. Error bars represent SEM between biological replicates.

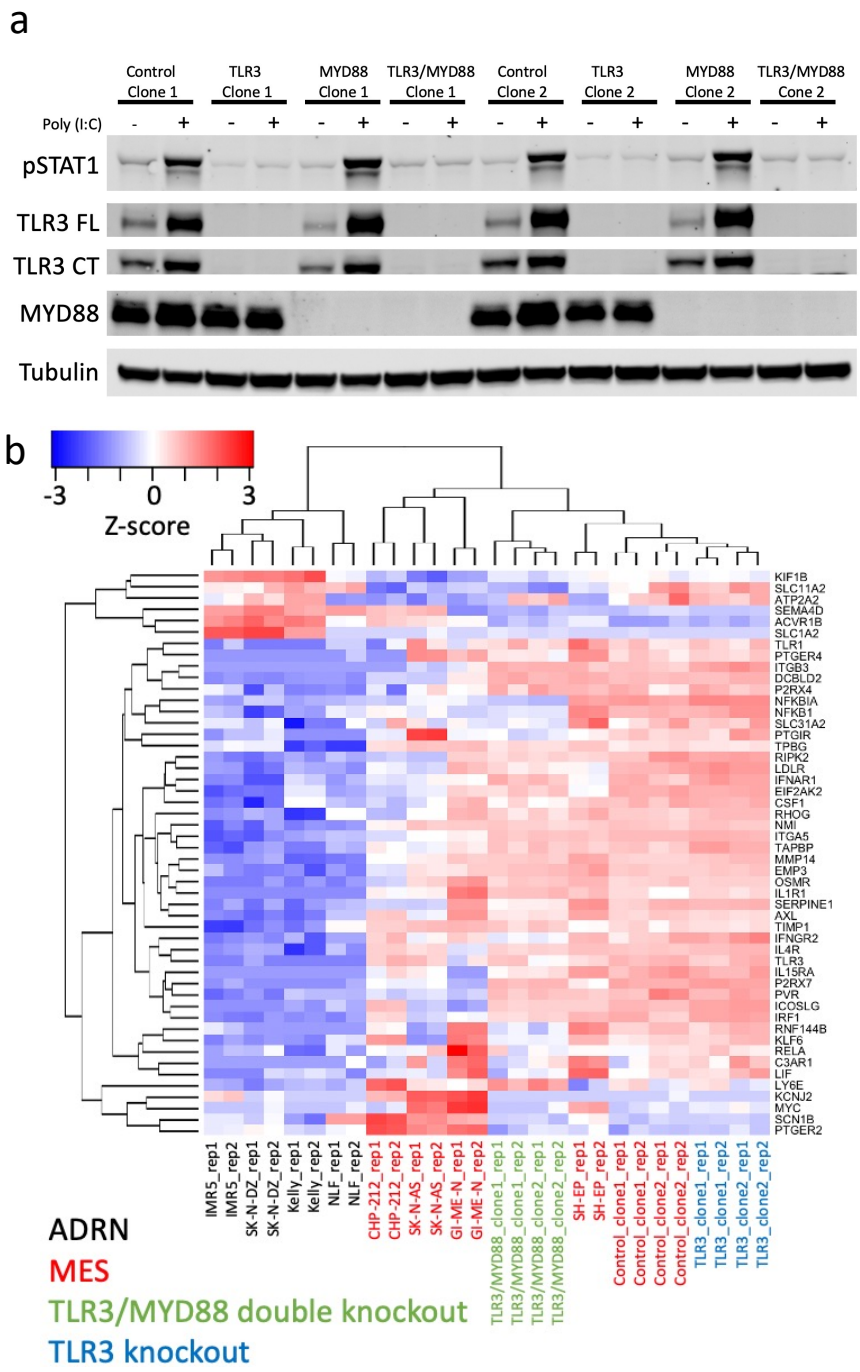

Fig. S13. TLR3 and MYD88 are not required for the enhanced inflammatory state in MES cells

a) Western blot showing the change in pSTAT1 after treatment with 30μg/mL of poly (I:C) for 24 hours in SH-EP MYCN-ER cells with either control sgRNAs (Luciferase and Rosa26), TLR3 knockout (sgRNAs against TLR3 and Rosa26), MYD88 knockout (sgRNAs against MYD88 and Luciferase), and TLR3/MYD88 double knockout. b) Heat map depicting the expression of the 50 genes in the Hallmark Inflammatory Response geneset that are most significantly different between ADRN (unresponsive) and MES (responsive) lines. Cell lines shown include MES and ADRN cell lines and SHEP-MYCN-ER cells with either control sgRNAs, knockout of TLR3, or

knockout of both TLR3 and MYD88. Western blots are representative of results from at least three separate experiments.

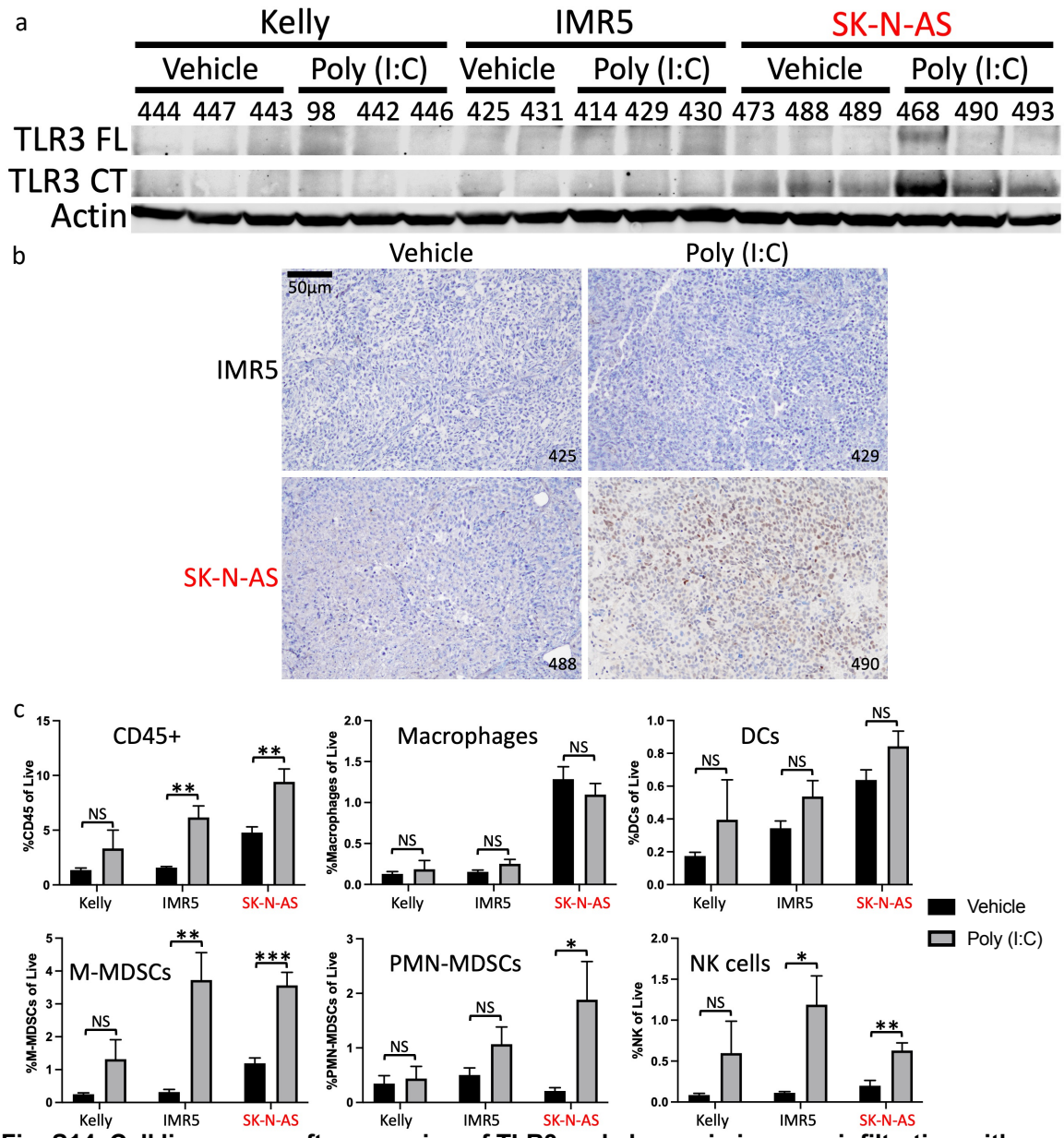

Fig. S14. Cell line xenograft expression of TLR3 and change in immune infiltration with poly (I:C)

a) Western blot showing TLR3 protein expression from xenograft tumors formed from the indicated cell lines collected 24 hours after intratumoral injection with saline control or 50µL of 1mg/mL of poly (I:C). Three separate tumors (numbers are tumor IDs) are shown for each treatment/cell line combination. Both the full length (FL) and active C-terminal fragment (CT) of TLR3 are shown. b) Immunohistochemical staining for pSTAT1 in the tumors derived from the indicated cell lines after the indicated treatments. Tumor IDs in the bottom right corner correspond to the western blot in (a). c) Change in relative infiltration of tumors formed from the indicated cell lines with the indicated immune cell types 24 hours after intratumoral injection with saline control or 50µL of 1mg/mL of poly (I:C). Immune cells identified using flow cytometry and calculated as percent of live cells. Two-tailed T-test, *p<0.05, **p<0.01, ***p<0.001.

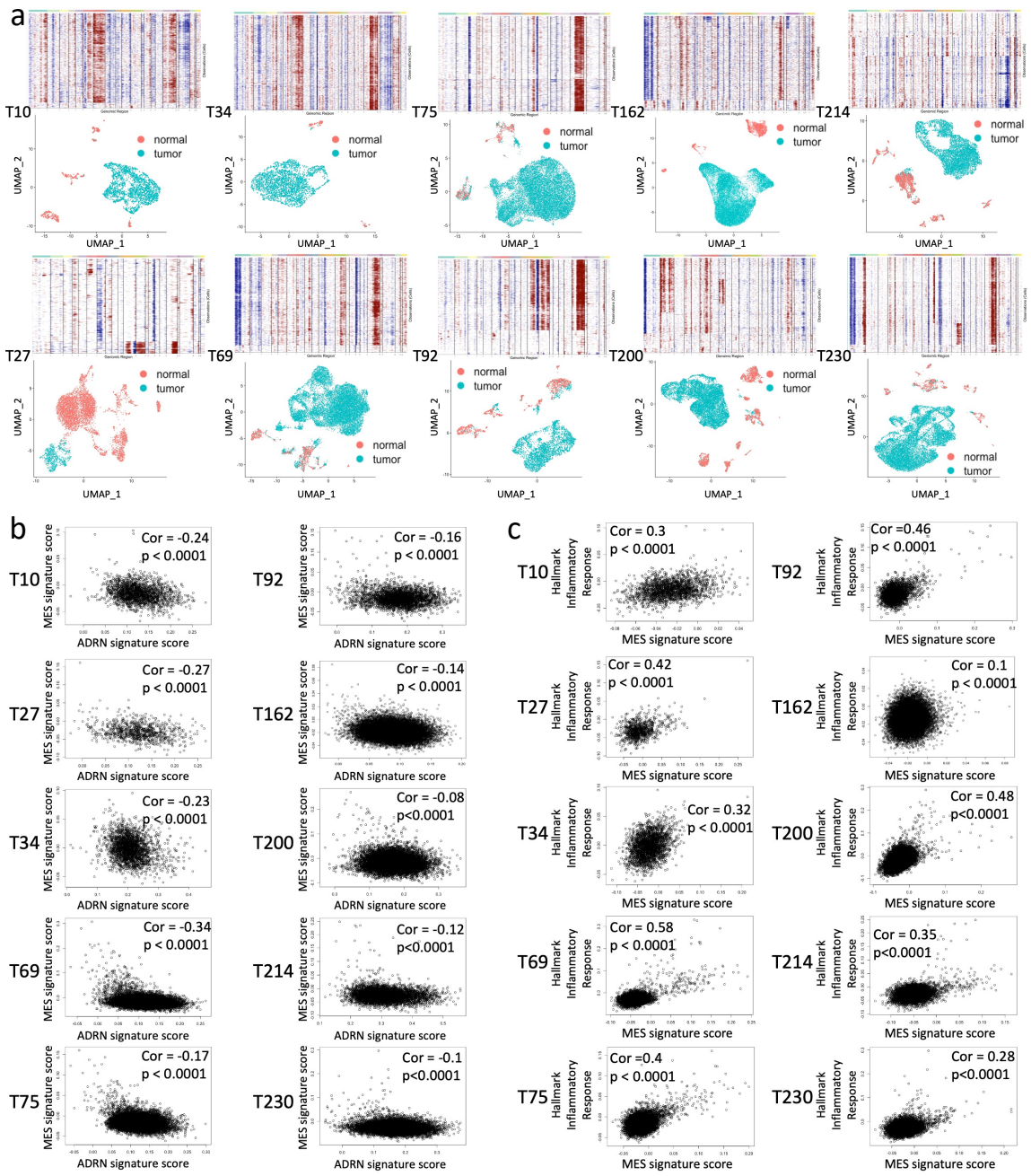

Fig. S15. scRNAseq analysis and data from individual tumors
a) For each sample, the top plot shows inferred CNV across for each cell (Y-axis) across chromosome location (X-axis). The bottom shows a UMAP plot for each sample with tumors cells assigned based on the CNV analysis in the above plot. Each sample is labelled to the left of the plots. b) Correlation between the MES and ADRN gene signatures (11) in the cells determined to be tumor based on CNV for each tumor sample. c) Correlation between the Hallmark Inflammatory Response signature (14) and the MES signature in the cells determined to be tumor based on CNV for each tumor sample.

Table S1. Correlations between Mesenchymal gene signatures and inflammatory sensing gene expression

	Versteeg dataset		Maris dataset		Tumor RNA-seq	
Gene name	**R-value**	**P-value**	**R-value**	**P-value**	**R-value**	**P-value**
TLR1	0.175	0.423	0.583	0.000122	0.696	2.06E-73
TLR2	0.046	0.836	0.505	0.00123	0.741	8.89E-88
TLR3	0.842	4.85E-07	0.61	0.0000478	0.738	8.56E-87
TLR4	0.65	0.000796	0.578	0.000143	0.753	3.22E-92
TLR5	0.158	0.472	-0.024	0.886	0.713	1.64E-78
TLR6	0.552	0.00635	0.557	0.000277	0.668	1.34E-65
TLR7	0.061	0.783	0.247	0.136	0.688	3.62E-71
TLR8	0.297	0.169	Not expressed	Not expressed	0.603	1.24E-50
TLR9	-0.028	0.901	-0.254	0.124	0.271	7.59E-10
MYD88	0.379	0.075	0.466	0.0032	0.458	3.67E-27
TBK1	0.175	0.424	0.752	5.31E-08	0.325	1.07E-13
TRIF/TICAM1	0.462	0.026	0.621	0.0000318	0.344	2.95E-15
IRAK1	0.427	0.042	0.306	0.062	0.028	0.53
IRAK2	0.629	0.00129	0.365	0.024	0.627	9.01E-56
IRAK4	0.609	0.00203	0.664	0.00000555	0.707	1.3E-76
TRAF3	0.165	0.453	0.332	0.041	0.233	1.51E-07
TRAF6	-0.495	0.016	0.153	0.359	-0.105	0.019
TRAM/TICAM2	0.683	0.000327	0.147	0.378	0.683	9.29E-70
SARM1	-0.711	0.000141	-0.059	0.726	-0.039	0.387
TIRAP	0.21	0.336	0.519	0.000849	0.123	0.0061
IKK alpha/CHUK	-0.067	0.76	0.673	0.00000368	0.109	0.015
IKK beta/IKBKB	0.364	0.088	0.736	1.43E-07	0.57	2.54E-44
IKK gamma/IKBKG	0.614	0.00183	0.764	2.38E-08	0.265	1.88E-09
IRF3	0.558	0.00568	0.727	0.00000024	0.599	9.42E-50
IRF7	0.119	0.587	0.359	0.027	0.451	2.51E-26
RELA	0.353	0.099	0.696	0.0000012	0.154	0.000577
RELB	0.642	0.000969	0.581	0.00013	0.625	3.21E-55
p50/NFKB1	5.98	0.00059	0.785	5.24E-09	0.673	6.67E-67
p52/NFKB2	0.484	0.019	0.77	1.6E-08	0.713	1.76E-78
IFNB1	0.015	0.946	0.497	0.00149	0.07	0.121
RIGI/DDX58	0.228	0.294	0.643	0.0000135	0.645	6.99E-60
MDA5/IFIH1	0.871	6.26E-08	0.551	0.000314	0.701	8.2E-75
cGAS/MB21D1	-0.148	0.5	0.018	0.915	0.73	3.92E-84
STING/TMEM173	0.586	0.0033	0.606	0.000055	0.864	5.94E-150
MAVS	0.182	0.405	0.57	0.000187	0.224	4.47E-07

Data obtained and analyzed within R2 (http://r2.amc.nl)

Table S2. Cell line sources and culture conditions

Cell line	Source	Culture Media
SH-EP	Michael Hogarty	DMEM, 10%FBS, 1%PS
SK-N-AS	Michael Hogarty	DMEM, 10%FBS, 1%PS
GI-ME-N	German Collection of Microorganisms and Cell Cultures (DSMZ)	DMEM, 10%FBS, 1%PS
CHP-212	John Maris	EMEM/F12 (1:1 mix), 10%FBS, 1%PS, 2mM L-Glutamine
SK-N-FI	John Maris	RPMI, 10% FBS, 1%PS, 2mM L-Glutamine
SK-N-SH	Michael Hogarty	RPMI, 10% FBS, 1%PS, 2mM L-Glutamine
ACN	Interlab Cell Line Collection (ICLC)	RPMI, 10% FBS, 1%PS, 2mM L-Glutamine, 1mM sodium pyruvate
NBEBc1	Michael Hogarty	RPMI, 10% FBS, 1%PS, 2mM L-Glutamine
LAN6	Michael Hogarty	RPMI, 10% FBS, 1%PS, 2mM L-Glutamine
NBL-S	John Maris	RPMI, 10% FBS, 1%PS, 2mM L-Glutamine
NB69	John Maris	RPMI, 10% FBS, 1%PS, 2mM L-Glutamine
Kelly	Michael Hogarty	DMEM, 10%FBS, 1%PS
NLF	Michael Hogarty	DMEM, 10%FBS, 1%PS
IMR-5	Michael Hogarty	DMEM, 10%FBS, 1%PS
IMR-32	Michael Hogarty	RPMI, 10% FBS, 1%PS, 2mM L-Glutamine
SK-N-DZ	John Maris	RPMI, 10% FBS, 1%PS, 2mM L-Glutamine
NB1643	Michael Hogarty	RPMI, 10% FBS, 1%PS, 2mM L-Glutamine
BE2(c)	Michael Hogarty	RPMI, 10% FBS, 1%PS, 2mM L-Glutamine
SH-SY-5Y	Michael Milone	DMEM, 10%FBS, 1%PS
CHLA-15	Michael Hogarty	IMDM, 20% FBS, 1% PS, 2mM L-Glutamine, 0.1% ITS premix (Insulin, Transferrin, Selenious Acid)
SH-EP MYCN-ER	Michael Hogarty	DMEM, 10%FBS, 1%PS
SK-N-AS MYCN-ER	Linda Valentijn	DMEM, 10%FBS, 1%PS
BE2c inducible shRNA	Marie Arsenian-Henriksson	EMEM/F12 (1:1 mix), 10%FBS, 1%PS, 1% Non-essential amino acids, 2mM L-Glutamine
THP-1	Alessandro Gardini	RPMI, 10%FBS, 1%PS

Table S3. Sources and sequences of reagents, antibodies, primers, and sgRNAs

Name	Source	Catalog number or sequence	Concentration (if applicable)
Poly (I:C)	Invivogen	tlrl-pic	30 μg/mL
Poly (I:C) Vaccigrade™	Invivogen	vac-pic	1mg/mL
LyoVec™-Poly (I:C)	Invivogen	tlrl-piclv	5 μg/mL (poly (I:C) component)
PAM3CSK4	Invivogen	tlrl-kit1hw	1 μg/mL
LTA-SA	Invivogen	tlrl-pslta	10 μg/mL
FLA-ST	Invivogen	tlrl-kit1hw	100 ng/mL
FSL-1	Invivogen	tlrl-kit1hw	4 μg/mL
Imiquimod	Invivogen	tlrl-kit1hw	5 μg/mL
ssRNA40	Invivogen	tlrl-kit1hw	5 μg/mL
LPS-EK	Invivogen	tlrl-kit1hw	1 μg/mL
ODN2006	Invivogen	tlrl-kit1hw	10 μg/mL
Recombinant IFNγ	Peprotech	300-02	20 ng/mL
Calf thymus DNA	Sigma	D1501	1μg/mL
Doxycycline	Sigma	D9891	50 ng/mL (inducible shRNA), 1μ/mL (PRRX1 expression)
4-hydroxytamoxifen	Sigma	H7904	500nM
Zeocin	Fisher	R25001	Optimized for each cell line
Puromycin	Fisher	A1113803	2.5 μg/mL (BE2(c)), 1μg/mL (CHP-212, NLF)
G418	Fisher	MT30234CR	500 μg/mL (Kelly, BE2(c)), 250 μg/mL (NLF)
MCP-1	Fisher	PHC1014	50nM
Matrigel	Corning	354230	50%
Nontargeting siRNA	Qiagen	1027280	30 pmol/well
MYCN siRNA_6	Qiagen	SI03113670	30 pmol/well
MYCN siRNA_7	Qiagen	SI03087518	30 pmol/well
NF-κB pNifty2-Luc	Invivogen	pnifty2-luc	
Myc-DDK-PRRX1a	Origene	RC213276	
Myc-DDK-TLR3	Origene	RC210497	
pLVX-TetOne	Takara	631847	
MART-1-IRES-GFP virus	Genecopoeia	G0616-Lv225	
LentiV_Cas9_neo	Dr. Junwei Shi		
LRG2.1T	Dr. Junwei Shi		
sgRNA TLR3_1	Integrated DNA Technologies (IDT)	TAAAGATAAGGAT TGGGTCT	
sgRNA TLR3_2	Integrated DNA Technologies (IDT)	CCCCCCCAAAAGT AGATACA	
sgRNA MYD88_1	Integrated DNA Technologies (IDT)	TGTCTCTGTTCTT GAACGTG	
sgRNA MYD88_2	Integrated DNA Technologies (IDT)	CTCGAGCAGTCG GCCTACAG	
sgRNA Rosa26	Integrated DNA Technologies (IDT)	GAAGATGGGCGG GAGTCTTC	

sgRNA Luciferase	Integrated DNA Technologies (IDT)	CACCGTTTGTGCAGCTGCTCGCCGG	
OAS1 qPCR primer_F	Integrated DNA Technologies (IDT)	GATGAGCTTGACATAGATTTGGG	
OAS1 qPCR primer_R	Integrated DNA Technologies (IDT)	GGTGGAGTTCGATGTGCTG	
TNFAIP3 qPCR primer_F	Integrated DNA Technologies (IDT)	CAAGTGGAACAGCTCGGATT	
TNFAIP3 qPCR primer_R	Integrated DNA Technologies (IDT)	GCCCAGGAATGCTACAGATAC	
RPLP0 qPCR primer_F	Integrated DNA Technologies (IDT)	TGTCTGCTCCCACAATGAAAC	
RPLP0 qPCR primer_R	Integrated DNA Technologies (IDT)	TCGTCTTTAAACCCTGCGTG	
Rabbit phospho-Tyr701 STAT1	Cell Signaling Technology	9167	1:1,000 (western blot), 1:100 (IHC)
Rabbit STAT1	Cell Signaling Technology	9172S	1:1,000
Mouse PHOX2A	Santa Cruz Biotechnology	sc-81978	1:500
Mouse PHOX2B	Santa Cruz Biotechnology	sc-376997	1:200
Mouse PRRX1	Origene	TA803116	1:2,000
Rabbit YAP	Cell Signaling Technology	14074	1:1,000
Rabbit TLR3	Cell Signaling Technology	6961	1:1,000
Rabbit SLUG (SNAI2)	Cell Signaling Technology	9585	1:1,000
Rabbit cGAS	Sigma	HPA031700	1:500
Rabbit DBH	Cell Signaling Technology	8586	1:1,000
Rabbit DLK1	Cell Signaling Technology	2069	1:1,000
Rabbit RIG-I	Cell Signaling Technology	3743	1:1,000
Rabbit MDA-5	Cell Signaling Technology	5321	1:1,000
Rabbit MYD88	Cell Signaling Technology	4283	1:1,000
Mouse α-tubulin	Calbiochem	CP06	1:10,000
Rabbit α-tubulin	Cell Signaling Technology	2144	1:1,000
Goat anti-rabbit Alexa Fluor 680 secondary antibody	Invitrogen	A21109	1:8,000
Goat anti-mouse Alexa Fluor 790 secondary antibody	Invitrogen	A11357	1:10,000
Goat anti mouse DyLight™ 800	Cell Signaling Technology	5257	1:15,000
PE-HLA-A,B,C antibody	Biolegend	311406	1:100
PE-Isotype control antibody	Biolegend	400214	1:100
Purified Rat Anti-Mouse CD16/CD32 (Mouse BD Fc Block™)	BD Biosciences	553141	1:100
LIVE/DEAD™ Fixable Aqua Dead Cell Stain Kit	Thermo Fisher Scientific	L34965	1:200
CD45 APC	Biolegend	103112	1:200
CD45 Alexa Fluor 700	Biolegend	103128	1:200
TCRβ FITC	Biolegend	109205	1:200
CD19 FITC	Biolegend	115505	1:200

CD11b BV785	Biolegend	101243	1:200
Ly6G APC Cy7	Biolegend	127623	1:200
Ly6C PerCpCy5.5	Biolegend	560525	1:200
F4/80 PE	eBioscience	12-4801-80	1:200
CD11c APC	BD Biosciences	561119	1:200
MHCII (I-A/I-E) BV605	Biolegend	107639	1:200
CD147 Alexa Fluor 647	Fisher	BDB562551	1:80
CD49b APC/Fire 750	Biolegend	108926	1:40
CD335 (NKp46)BV 421	Biolegend	137611	1:80

SI References

1. Z. E. Walton *et al.*, Acid Suspends the Circadian Clock in Hypoxia through Inhibition of mTOR. *Cell* **174**, 72-87 e32 (2018).
2. J. D. Buenrostro, P. G. Giresi, L. C. Zaba, H. Y. Chang, W. J. Greenleaf, Transposition of native chromatin for fast and sensitive epigenomic profiling of open chromatin, DNA-binding proteins and nucleosome position. *Nat Methods* **10**, 1213-1218 (2013).
3. M. R. Corces *et al.*, An improved ATAC-seq protocol reduces background and enables interrogation of frozen tissues. *Nat Methods* **14**, 959-962 (2017).
4. K. Upton *et al.*, Epigenomic profiling of neuroblastoma cell lines. *Sci Data* **7**, 116 (2020).
5. B. Langmead, C. Trapnell, M. Pop, S. L. Salzberg, Ultrafast and memory-efficient alignment of short DNA sequences to the human genome. *Genome Biol* **10**, R25 (2009).
6. S. Heinz *et al.*, Simple combinations of lineage-determining transcription factors prime cis-regulatory elements required for macrophage and B cell identities. *Mol Cell* **38**, 576-589 (2010).
7. M. I. Love, W. Huber, S. Anders, Moderated estimation of fold change and dispersion for RNA-seq data with DESeq2. *Genome Biol* **15**, 550 (2014).
8. J. L. Harenza *et al.*, Transcriptomic profiling of 39 commonly-used neuroblastoma cell lines. *Sci Data* **4**, 170033 (2017).
9. J. L. Rokita *et al.*, Genomic Profiling of Childhood Tumor Patient-Derived Xenograft Models to Enable Rational Clinical Trial Design. *Cell reports* **29**, 1675-1689 e1679 (2019).
10. L. J. Valentijn *et al.*, Functional MYCN signature predicts outcome of neuroblastoma irrespective of MYCN amplification. *Proceedings of the National Academy of Sciences of the United States of America* **109**, 19190-19195 (2012).
11. T. van Groningen *et al.*, Neuroblastoma is composed of two super-enhancer-associated differentiation states. *Nature genetics* **49**, 1261-1266 (2017).
12. W. Zhang *et al.*, Comparison of RNA-seq and microarray-based models for clinical endpoint prediction. *Genome Biol* **16**, 133 (2015).
13. V. Boeva *et al.*, Heterogeneity of neuroblastoma cell identity defined by transcriptional circuitries. *Nature genetics* **49**, 1408-1413 (2017).
14. A. Liberzon *et al.*, The Molecular Signatures Database (MSigDB) hallmark gene set collection. *Cell Syst* **1**, 417-425 (2015).